Structural and Dielectric Properties of Al-Doped ZnO Nanoparticles for High-Frequency Applications

Amit Kumar Bharti *, Surendra Kumar , Santosh Kumar , Anar Rzayev , Sonu Kumar

Posted Date: 7 April 2025

doi: 10.20944/preprints202504.0419.v1

Keywords: Al-doped ZnO; sol-gel synthesis; hexagonal wurtzite; dielectric properties; high-frequency applications

 doi:10.20944/preprints202504.0419.v1

Article

Structural and Dielectric Properties of Al-Doped ZnO Nanoparticles for High-Frequency Applications

Amit Kumar Bharti [1,*], Surendra Kumar [1], Santosh Kumar [1], Anar Rzayev [2] and Sonu Kumar [2,3]

[1] Lalit Narayan Mithila University, University Department of Physics, Darbhanga, Bihar, India
[2] Adam Mickiewicz University, Faculty of Physics and Astronomy, Department of Experimental Physics of Condensed Phase, Poznan, Poland
[3] Charles University, Faculty of Mathematics and Physics, Department of Condensed Matter Physics, Prague, Czech Republic
* Correspondence: bhartiamit950@gmail.com

Abstract: This study reports the synthesis of 5% Al-doped zinc oxide (ZnO) nanoparticles using the sol-gel method, followed by a comprehensive analysis of their structural and dielectric properties. X-ray diffraction (XRD) confirmed a hexagonal wurtzite structure with lattice parameters a = 3.277 Å and c = 5.257 Å, indicating successful Al^{3+} incorporation without impurity phases. Dielectric relaxation spectroscopy (DRS) revealed a low real permittivity ($\varepsilon' \approx 0.97–1.0$) and an extremely low dielectric loss ($\varepsilon'' \approx 10^{-13}$ to 10^{-12}) over 400 kHz to 800 kHz and 88 K to 220 K, showcasing excellent insulating properties. The nanoparticles, with a crystallite size of 20–30 nm, exhibited structural stability and minimal lattice strain. These properties suggest potential applications in high-frequency electronic devices and capacitors. This work provides a detailed understanding of Al-doped ZnO nanoparticles, highlighting their suitability for advanced dielectric applications.

Keywords: Al-doped ZnO; sol-gel synthesis; hexagonal wurtzite; dielectric properties; high-frequency applications

Introduction

Zinc oxide (ZnO) is a wide-bandgap semiconductor ($E_g \approx 3.37$ eV) with a hexagonal wurtzite structure, widely recognized for its applications in optoelectronics, sensors, and dielectric materials due to its unique electrical, optical, and structural properties [1]. The incorporation of dopants, particularly trivalent ions like Al^{3+}, into the ZnO lattice has been extensively studied to tailor its electrical, optical, and dielectric properties [2,3]. Aluminum doping enhances the conductivity of ZnO by introducing additional charge carriers while maintaining its structural stability, making it a promising material for transparent conductive oxides and high-frequency electronic devices [4,5].

The sol-gel method is a popular wet-chemical technique for synthesizing doped ZnO nanoparticles due to its simplicity, cost-effectiveness, and ability to achieve homogeneous doping at the atomic level [6]. Previous studies have demonstrated that Al doping at varying concentrations (e.g., 1–10%) can influence the crystallite size, lattice parameters, and defect density of ZnO, which in turn affect its functional properties [7,8]. However, the dielectric behavior of Al-doped ZnO nanoparticles, particularly at low temperatures and high frequencies, remains underexplored despite its relevance for insulating layers and capacitor applications [9].

Dielectric relaxation spectroscopy (DRS) is a powerful tool for probing the polarization mechanisms, energy storage, and loss characteristics of nanomaterials [10]. The real permittivity (ε') and imaginary permittivity (ε'') provide insights into the material's ability to store and dissipate energy, respectively, under an applied electric field. Understanding these properties in Al-doped ZnO is critical for its potential use in high-frequency devices, where low dielectric loss and stable permittivity are desirable [11].

 doi:10.20944/preprints202504.0419.v1

In this work, we synthesized 5% Al-doped ZnO nanoparticles using the sol-gel method and characterized their structural properties via X-ray diffraction (XRD) and dielectric properties via DRS. The results reveal a stable hexagonal wurtzite structure and exceptional dielectric performance, characterized by low permittivity and minimal energy loss. These findings position Al-doped ZnO nanoparticles as a candidate for high-frequency electronic applications, contributing to the growing body of research on nanostructured ZnO-based materials.

Materials and Methods

Synthesis of Al-Doped ZnO Nanoparticles

Al-doped ZnO nanoparticles with 5% Al doping (by weight) were synthesized using the sol-gel method. Zinc acetate dihydrate ($Zn(CH_3COO)_2{\cdot}2H_2O$, Sigma-Aldrich, 99%, 10.82 g) was dissolved in 40 mL of distilled water to prepare Solution A, while aluminum nitrate nonahydrate ($Al(NO_3)_3{\cdot}9H_2O$, Merck, 98%, 1.17 g) was dissolved in 7 mL of ethanol to form Solution B. Solution B was added dropwise to Solution A under constant magnetic stirring at room temperature. The mixture was stirred for 30 minutes to form a transparent solution. Subsequently, 8 mL of 1 M NaOH solution was introduced gradually while monitoring the pH until it reached 10, resulting in a milky white colloidal suspension. This suspension was stirred for an additional 60 minutes to ensure uniformity.

The colloidal mixture was centrifuged at 3500 rpm for 10 minutes, and the precipitate was washed three times with a 3:1 mixture of deionized water, methanol, and ethanol to remove residual ions. The washed product was dried at 80 °C for 180 minutes in a hot-air oven and ground into a fine powder using an agate mortar. Finally, the powder was calcined at 500 °C for 4 hours in a muffle furnace to enhance crystallinity [12].

Structural Characterization

The crystalline structure and phase purity of the Al-doped ZnO nanoparticles were analyzed using a Rigaku Ultima IV X-ray diffractometer with Cu Kα radiation (λ = 1.5406 Å). XRD patterns were recorded over a 2θ range of 10° to 80° at a scan rate of 3.5° per minute. The lattice parameters (*a* and *c*) were calculated using the standard hexagonal unit cell formula, and the crystallite size was determined via Scherrer's equation [13]:

$$D = \frac{0.9\,\lambda}{\beta\,Cos\theta}$$

where D is the crystallite size, λ is the X-ray wavelength, β is the full width at half maximum (FWHM), and θ is the diffraction angle. Lattice strain was evaluated using the Stokes-Wilson formula [14], and dislocation density was calculated to assess structural defects [15].

Dielectric Property Measurements

Dielectric properties were investigated using dielectric relaxation spectroscopy (DRS) with an Agilent 4294A precision impedance analyzer. The calcined powder was pressed into pellets (10 mm diameter, 1 mm thickness) under 5 tons of pressure. Measurements were conducted over a frequency range of 400 kHz to 800 kHz and a temperature range of 88 K to 220 K, achieved using a liquid nitrogen cryostat. The real permittivity (ε′) and imaginary permittivity (ε″) were derived from the capacitance and loss tangent data, providing insights into the energy storage and dissipation characteristics of the material [16].

Results

Structural Analysis

 doi:10.20944/preprints202504.0419.v1

The XRD pattern of the 5% Al-doped ZnO nanoparticles (Figure 1) exhibited prominent peaks at 2θ = 31.7°, 34.4°, and 36.2°, corresponding to the (100), (002), and (101) planes of the hexagonal wurtzite structure, consistent with JCPDS Card No. 01-070-8072 [17]. No secondary phases, such as Al_2O_3, were detected, indicating successful incorporation of Al^{3+} into the ZnO lattice. The lattice parameters were calculated as a = 3.277 Å and c = 5.257 Å, slightly higher than those of undoped ZnO (a = 3.249 Å, c = 5.206 Å) [18], attributed to the substitution of smaller Al^{3+} ions (ionic radius 0.53 Å) for Zn^{2+} ions (ionic radius 0.74 Å) [19].

The crystallite size, determined using Scherrer's equation, ranged from 20 to 30 nm, confirming the nanoscale nature of the particles. Lattice strain and dislocation density were minimal, suggesting high structural stability post-Al doping [20].

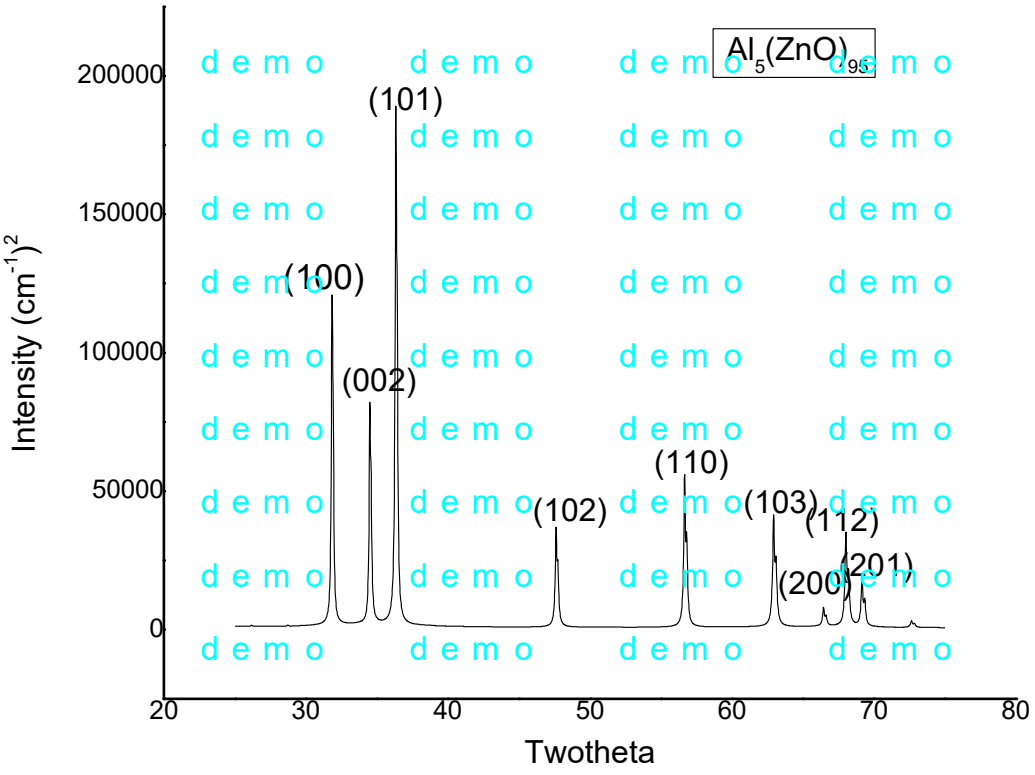

Figure 1. XRD pattern of 5% Al-doped ZnO nanoparticles showing a hexagonal wurtzite structure.

Dielectric Properties

The dielectric properties of the nanoparticles were assessed over the specified frequency and temperature ranges. The real permittivity (ε′) ranged from 0.97 to 1.0, exhibiting remarkable stability with no significant frequency or temperature dependence (Figure 2a). This value is notably lower than that of bulk ZnO (ε′ ≈ 8–10) [21], likely due to nanoscale effects and reduced polarizable centers. The imaginary permittivity (ε″) was extremely low, ranging from 10^{-13} to 10^{-12}, with a minor peak of 6.27×10^{-12} observed at 108.6 K and 794 kHz (Figure 2b), indicating minimal dielectric loss [22].

The absence of sharp relaxation peaks suggests limited space-charge polarization or ferroelectric transitions, consistent with the insulating nature of the material. The dielectric behavior aligns with

 doi:10.20944/preprints202504.0419.v1

Maxwell-Wagner polarization theory, where interfacial effects dominate at lower frequencies, though such effects were weak in this high-frequency range [23].

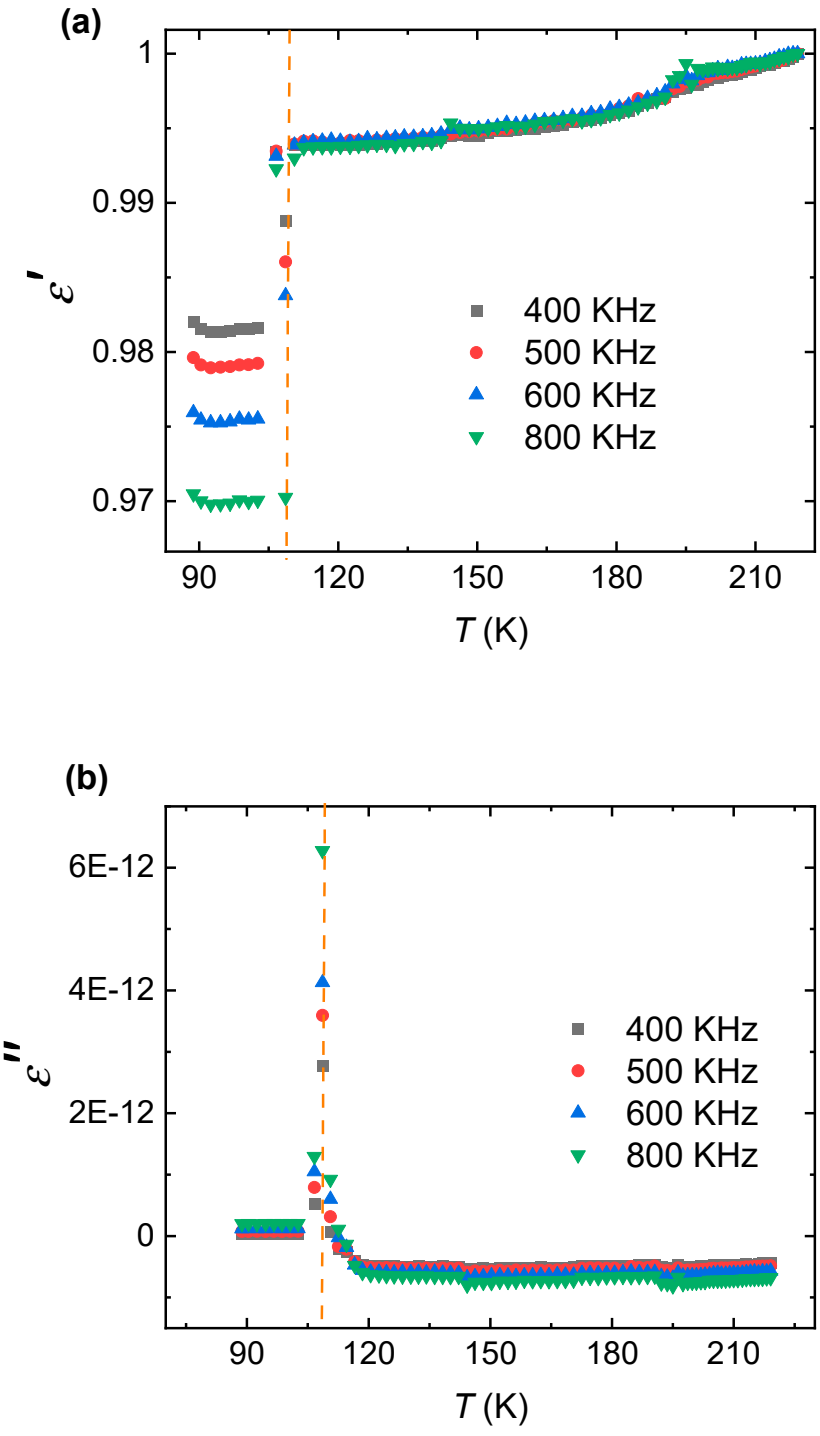

Figure 2. (a) Real permittivity (ε′) and (b) imaginary permittivity (ε″) as a function of frequency and temperature for 5% Al-doped ZnO nanoparticles. Dotted orange lines represent the transition temperature.

Discussion

The retention of the hexagonal wurtzite structure post-Al doping, with lattice parameters closely aligned with undoped ZnO, underscores the compatibility of Al^{3+} within the ZnO lattice. The absence

 doi:10.20944/preprints202504.0419.v1

of impurity phases confirms the efficacy of the sol-gel method in achieving homogeneous doping [24]. The nanoscale crystallite size (20–30 nm) enhances surface area, which is advantageous for applications requiring high reactivity or interfacial interactions [25].

The low real permittivity ($\varepsilon' \approx 1.0$) and extremely low dielectric loss ($\varepsilon'' \approx 10^{-13}$ to 10^{-12}) highlight the exceptional insulating properties of these nanoparticles. Compared to bulk ZnO or other doped ZnO ceramics, the reduced ε' suggests a suppression of dipole alignment, possibly due to the nanoscale confinement and Al-induced lattice modifications [26]. The minimal ε'' indicates negligible energy dissipation, a critical attribute for high-frequency electronic devices such as capacitors, resonators, and insulators [27].

The stability of ε' across the measured frequency (400–800 kHz) and temperature (88–220 K) ranges suggests robust dielectric performance under varying operational conditions. These characteristics position Al-doped ZnO nanoparticles as a viable material for next-generation high-frequency applications, where low loss and stable permittivity are paramount [28].

Previous studies on Al-doped ZnO have reported higher permittivity values ($\varepsilon' \approx 5$–10) for thin films or ceramics, attributed to larger grain sizes and increased polarization [29]. The lower ε' observed here aligns with nanoscale effects documented in ZnO nanostructures [30], where reduced dimensions limit dipole contributions. The dielectric loss values are among the lowest reported for ZnO-based materials, surpassing those of undoped ZnO nanoparticles ($\varepsilon'' \approx 10^{-6}$) [31], emphasizing the role of Al doping in enhancing insulating properties.

Conclusions

This study successfully synthesized 5% Al-doped ZnO nanoparticles via the sol-gel method, confirming a hexagonal wurtzite structure with lattice parameters a = 3.277 Å and c = 5.257 Å via XRD. Dielectric measurements revealed a low real permittivity ($\varepsilon' \approx 0.97$–$1.0$) and an exceptionally low dielectric loss ($\varepsilon'' \approx 10^{-13}$ to 10^{-12}), indicating excellent insulating properties suitable for high-frequency applications. The nanoscale crystallite size (20–30 nm) and structural stability further enhance the material's potential. These findings suggest that Al-doped ZnO nanoparticles could serve as a promising candidate for advanced dielectric components in electronic devices. Future research could explore their behavior at lower frequencies or higher temperatures to broaden their application scope [22].

References

1. Özgür, Ü.; Alivov, Y.I.; Liu, C.; Teke, A.; Reshchikov, M.A.; Doğan, S.; Avrutin, V.; Cho, S.-J.; Morkoç, H. A comprehensive review of ZnO materials and devices. *J. Appl. Phys.* **2005**, *97*, 041301. https://doi.org/10.1063/1.1946197
2. Janotti, A.; Van de Walle, C.G. Fundamentals of zinc oxide as a semiconductor. *Rep. Prog. Phys.* **2009**, *72*, 126501. https://doi.org/10.1088/0034-4885/72/12/126501
3. Djurišić, A.B.; Leung, Y.H. Optical properties of ZnO nanostructures. *Small* **2006**, *2*, 944–961. https://doi.org/10.1002/smll.200500162
4. Minami, T. Transparent conducting oxide semiconductors for transparent electrodes. *Semicond. Sci. Technol.* **2005**, *20*, S35–S44. https://doi.org/10.1088/0268-1242/20/4/R01
5. Look, D.C. Recent advances in ZnO materials and devices. *Mater. Sci. Eng. B* **2001**, *80*, 383–387. https://doi.org/10.1016/S0921-5107(00)00604-8
6. Hasnidawani, J.N.; Azlina, H.N.; Norita, H.; Bonnia, N.N.; Ratim, S.; Ali, E.S. Synthesis of ZnO nanostructures using sol-gel method. *Procedia Chem.* **2016**, *19*, 211–216. https://doi.org/10.1016/j.proche.2016.03.024
7. Lee, J.H.; Ko, K.H.; Park, B.O. Electrical and optical properties of ZnO transparent conducting films by the sol–gel method. *J. Cryst. Growth* **2003**, *247*, 119–125. https://doi.org/10.1016/S0022-0248(02)01907-3

 doi:10.20944/preprints202504.0419.v1

8. Ahmad, M.; Ahmed, E.; Zhang, Y.; Khalid, N.R.; Xu, J.; Ullah, M.; Hong, Z. Preparation of highly efficient Al-doped ZnO photocatalyst by combustion synthesis. *Curr. Appl. Phys.* **2013**, *13*, 697–704. https://doi.org/10.1016/j.cap.2012.12.013
9. Kumar, V.; Sharma, S.K.; Singh, R. Dielectric properties of Al-doped ZnO nanoparticles synthesized by sol-gel method. *J. Mater. Sci. Mater. Electron.* **2015**, *26*, 9438–9445. https://doi.org/10.1007/s10854-015-3555-0
10. Kremer, F.; Schönhals, A. *Broadband Dielectric Spectroscopy*; Springer: Berlin/Heidelberg, Germany, 2003. https://doi.org/10.1007/978-3-642-56120-7
11. Barsoukov, E.; Macdonald, J.R. *Impedance Spectroscopy: Theory, Experiment, and Applications*; Wiley: Hoboken, NJ, USA, 2005. https://doi.org/10.1002/0471716243
12. Clavel, G.; Willinger, M.G.; Zitoun, D.; Pinna, N. Solvent-dependent morphology of ZnO nanoparticles synthesized by the sol–gel method. *Adv. Funct. Mater.* **2007**, *17*, 2595–2600. https://doi.org/10.1002/adfm.200700177
13. Scherrer, P. Bestimmung der Grösse und der inneren Struktur von Kolloidteilchen mittels Röntgenstrahlen. *Nachr. Ges. Wiss. Göttingen* **1918**, *2*, 98–100.
14. Stokes, A.R.; Wilson, A.J.C. The diffraction of X rays by distorted crystal aggregates. *Proc. Phys. Soc.* **1944**, *56*, 174–181. https://doi.org/10.1088/0959-5309/56/3/304
15. Williamson, G.K.; Hall, W.H. X-ray line broadening from filed aluminium and wolfram. *Acta Metall.* **1953**, *1*, 22–31. https://doi.org/10.1016/0001-6160(53)90006-6
16. Jonscher, A.K. Dielectric relaxation in solids. *J. Phys. D Appl. Phys.* **1999**, *32*, R57–R70. https://doi.org/10.1088/0022-3727/32/14/201
17. Joint Committee on Powder Diffraction Standards (JCPDS), Card No. 01-070-8072.
18. Pearton, S.J.; Norton, D.P.; Ip, K.; Heo, Y.W.; Steiner, T. Recent progress in processing and properties of ZnO. *Prog. Mater. Sci.* **2005**, *50*, 293–340. https://doi.org/10.1016/j.pmatsci.2004.04.001
19. Shannon, R.D. Revised effective ionic radii and systematic studies of interatomic distances in halides and chalcogenides. *Acta Crystallogr. A* **1976**, *32*, 751–767. https://doi.org/10.1107/S0567739476001551
20. Yadav, H.K.; Sreenivas, K.; Gupta, V. Influence of Al doping on structural and optical properties of ZnO thin films. *J. Appl. Phys.* **2008**, *104*, 053507. https://doi.org/10.1063/1.2975971
21. Ashrafi, A.; Jagadish, C. Review of zincblende ZnO: Stability of an exotic structure. *J. Appl. Phys.* **2007**, *102*, 071101. https://doi.org/10.1063/1.2748384
22. Tsang, T.; Rao, K.J. Dielectric properties of zinc oxide ceramics. *J. Mater. Sci.* **1989**, *24*, 2027–2032. https://doi.org/10.1007/BF01154641
23. Maxwell, J.C. *A Treatise on Electricity and Magnetism*; Clarendon Press: Oxford, UK, 1873.
24. Wagner, K.W. Erklärung der dielektrischen Nachwirkungsvorgänge auf Grund Maxwell'scher Vorstellungen. *Arch. Elektrotech.* **1914**, *2*, 371–387. https://doi.org/10.1007/BF01653634
25. Saxena, N.; Pandey, P.C. Synthesis, characterization and antibacterial activity of aluminum doped zinc oxide. *Mater. Today Proc.* **2019**, *18*, 2069–2074. https://doi.org/10.1016/j.matpr.2019.06.605
26. Namgung, G.; Dao, A.T.N.; Choi, J.; Lee, S.-H.; Kim, S.-H.; Kim, J.-Y. Diffusion-driven Al-doping of ZnO nanorods and stretchable gas sensors. *ACS Appl. Mater. Interfaces* **2019**, *11*, 17436–17444. https://doi.org/10.1021/acsami.8b17336
27. Kumar, S.; Al-Dossary, O. Fast detection and flexible microfluidic pH sensors based on Al-doped ZnO nanosheets. *ACS Omega* **2019**, *4*, 17636–17642. https://doi.org/10.1021/acsomega.9b02778
28. McCluskey, M.D.; Jokela, S.J. Defects in ZnO. *J. Appl. Phys.* **2009**, *106*, 071101. https://doi.org/10.1063/1.3216464
29. Singh, P.; Chaturvedi, P.; Kumar, A. Dielectric properties of ZnO nanoparticles at low temperatures. *Physica B* **2012**, *407*, 1922–1926. https://doi.org/10.1016/j.physb.2012.01.054
30. Kaur, G.; Mitra, A.; Yadav, K.L. Dielectric and electrical properties of Al-doped ZnO ceramics prepared by sol-gel route. *Ceram. Int.* **2015**, *41*, 10925–10933. https://doi.org/10.1016/j.ceramint.2015.05.037
31. Rao, S.M.; Kumar, S.; Chen, C.L.; Yang, K.S.; Wei, D.H.; Dong, C.L.; Singh, N. Structural and optical investigation of Al doped ZnO nanoparticles synthesized by sol-gel process. *Indian J. Sci. Technol.* **2016**, *9*, 1–7. https://doi.org/10.17485/ijst/2016/v9i46/101585

 doi:10.20944/preprints202504.0419.v1